PHYSICAL REVIEW B **79**, 035308 (2009)

Universal aspects of photocurrent-voltage characteristics in dye-sensitized nanocrystalline TiO_2 photoelectrochemical cells

J. S. Agnaldo,[1] J. C. Cressoni,[1] and G. M. Viswanathan[1,2]

[1]*Laboratório de Energia Solar, Núcleo de Tecnologias e Sistemas Complexos, Instituto de Física,*
Universidade Federal de Alagoas, Maceió-AL 57072-970, Brazil
[2]*Consortium of the Americas for Interdisciplinary Science, University of New Mexico, 800 Yale Boulevard NE,*
Albuquerque, New Mexico 87131, USA

(Received 29 August 2008; published 9 January 2009)

We propose a linearizable model for the nonlinear photocurrent-voltage characteristics of dye-sensitized nanocrystalline TiO_2 photoelectrochemical solar cells. We solve the model and report theoretically predicted values for fill factors. A single free parameter of the model controls the fill factor. Upon renormalization, diverse experimental current-voltage data collapse onto a single universal function. The theoretical underpinning provides insight into physical mechanisms responsible for the large fill factors as well as their known dependence on the open circuit voltage. These advances allow the estimation of the complete current-voltage curve and fill factor from any three experimental data points, e.g., the open circuit voltage, the short circuit current, and one other intermediate measurement.

DOI: 10.1103/PhysRevB.79.035308 PACS number(s): 84.60.Jt, 05.40.−a, 72.80.Le, 85.60.−q

I. INTRODUCTION

The concepts of scaling, universality, and renormalization[1] led to advances in the study of phase transitions and critical phenomena[2] and more recently to important advances[3] in many other fields: random walks and anomalous diffusion,[4–10] finance and economics,[11] networks,[12] movement ecology,[13,14] heartbeat dynamics,[15] and even music.[16] Here we address the problem of the current-voltage characteristics of a major class of solar cells using the concepts of scaling, universality, and renormalization. Continuous-time random-walk models[17] with sublinear scaling[18] of the mean-square displacement with time have successfully found application[10] in describing experimentally measured features of dye-sensitized solar cells.[19,20]

An important feature of photovoltaic solar cells and of diverse optoelectronic devices studied in semiconductor physics concerns their current-voltage characteristics.[21,22] Previous theoretical and experimental studies of dye-sensitized solar cells[19] have identified the dependence of the photocurrent and photovoltage on radiant power,[23] but not the precise nonlinear dependence of the photocurrent on the photovoltage under conditions of constant radiant power. Variability in the manufacturing process includes the choice of dye, the sintering temperature, thickness of the nanoporous TiO_2 film, and choice of chemical treatments. This diversity leads to significant qualitative and quantitative variation in photocurrent-voltage characteristics and of the relevant quantities such as the open circuit voltage V_{oc} or the short circuit current density J_{sc}. Variation occurs also in important quantities known as *fill factors* (FF), defined as the largest possible power output per unit area divided by $J_{sc}V_{oc}$. Such variability has discouraged attempts to identify (possibly "hidden") dynamical patterns that could yield important insights into the regenerative photoelectrochemical mechanisms that underlie the conversion process. Given the variability and diversity in the characteristics, which properties remain universal and which nonuniversal? More importantly from an experimental point of view, how can we quantitatively model the photocurrent-voltage characteristics, based on fundamental principles? Here we answer these questions by deriving an analytical expression for the photocurrent.

This article is organized as follows. In Sec. II we develop a general linearizable model of dye-sensitized solar cells. In this section we also discuss the physical significance of a constitutive equation that we introduce to try to capture the universal aspects of dye solar cells while also allowing for wide variation in the specific properties. In Sec. III we report the results comparing theory and experiment. Finally, in Sec. IV we discuss our results in quantitative terms and report our conclusions.

II. LINEARIZABLE MODEL OF DYE SOLAR CELLS

The topic of solar energy in general[24] and dye solar cells in particular[10,19,23,25–30]attracts broad interest from diverse sectors of society due to technological, economic, political, and environmental considerations. The scientific interest in dye-sensitized TiO_2 solar cells stems from their unusual features and mode of operation: (i) efficient charge separation due to ultrafast injection of electron from the dye on picosecond and subpicosecond time scales;[27,30] (ii) conduction consisting only of injected electrons rather than electron-hole pairs,[19] due to the wide band gap of the semiconductor TiO_2; (iii) high optical density due to the large surface area of the dye-sensitized nanoporous semiconductor;[27] (iv) negligible charge recombination with the oxidized dye;[19,23] and (v) high quantum yields.[27]

We approach the nonlinear photocurrent-voltage characteristics of TiO_2 dye-sensitized solar cells from the point of view of universality. The idea of universality[1] most commonly brings to mind the fact that critical exponents of phase transitions do not depend on the details of the microscopic dynamics for large classes of systems. However, the concept of universality is much older, e.g., Gaussian or "normal" statistics was until not too long ago considered universal and remains to this day ubiquitous, due to the wide (but not universal) applicability of the central limit theorem. Whenever some property is universal (e.g., critical exponents or probability density functions), suitable rescalings or transformations can highlight or "bring out" the universality of the property, such that all the data points for a variety of different systems "collapse" onto a single (possibly generalized) function. Although the technique of data collapse initially became widespread in the field of critical phenomena,[2] it has since found application[3] in the study of nonlinear dynamical systems and complex systems, e.g., finance,[11] human heartbeat dynamics,[15] and the physics of foraging.[13,14] The key advantage that such techniques confer to the interpretation of experimental data stems from the possibility of quantitatively describing diverse systems and phenomena using very few free parameters.

We will show below, using a proposed model, that the rescaled current-voltage experimental data collapse onto a single universal function for a variety of different solar cells (despite the inherently quantum-mechanical nature of the photoelectrochemical process underlying the operation of dye-sensitized cells). The model also allows us to predict values of the fill factors. Most importantly, the conceptual advance enables us to estimate the complete current-voltage curve and fill factor from any three experimental data points. Typically, these data points will be the open circuit voltage, the short circuit current, and one other intermediate measurement along the current-voltage curve. We expect our results to become immediately useful in modeling photocurrent-voltage characteristics of real dye-sensitized solar cells.

In what follows, we briefly describe the essential features of dye solar cells. We take as our starting point a textbook description of electrochemical processes close to equilibrium. Although one cannot *a priori* assume a well-mixed liquid at nanoscopic scales, the validity of this approach has previously been generalized and extended to nanocrystalline dye-sensitized solar cells by Huang *et al.*[23] We then add a phenomenologically motivated constitutive equation that introduces a finely tuned characteristic voltage (or energy) scale. This ingredient in the model introduces a degree of variability into the description of the system. However, it also captures the essential behavior that (we expect) remains approximately universal. Finally, we solve and simplify the resulting set of equations by making empirically acceptable approximations. This leads to our main results, which fit the experimental data remarkably well.

A. Charge separation and recombination

We briefly summarize the operation of dye-sensitized solar cells. The devices consist of a nanoporous semiconductor TiO_2 film sensitized by adsorbed charge-transfer dyes in contact with a nonaqueous electrolyte. When a crystalline semiconductor with a more negative Fermi level makes contact with an electrolyte with a more positive redox potential, electrons flow from the semiconductor to the solution in a manner analogous to what takes place in a *p*-*n* junction when a depletion layer forms. After the initial equilibration, the depletion layer together with Helmholtz and Gouy-Chapman layers in the electrolyte form a space-charge layer at the interface, bending the edges of the valence and conduction bands upwards, such that the Fermi level and redox potential remain the same across the semiconductor-electrolyte interface at all points. This space-charge layer allows charge separation to proceed as follows: visible light excites an electron within the dye molecule, causing injection of the electron into the conduction band of the semiconductor and away from the electrolyte interface. Subsequently, the dye cation becomes reduced by a redox couple in the nonaqueous electrolyte, typically, a solution with electroactive donor iodide (I^-) and acceptor tri-iodide (I_3^-) ions. A glass electrode with transparent conducting oxide makes contact with the semiconductor while a counterelectrode (typically made of Pt) returns the electrons to the electrolyte—thus closing the circuit and allowing a current to flow.

Although a similar equilibration occurs for a nanocrystalline semiconductor, the very small size of TiO_2 nanoparticles in fact prevents a significant depletion region from forming.[20] Under reverse bias, the voltage drop is only a few mV, leading to negligible electric fields.[20] This result, confirmed by Hodes, Howell, and Peter,[31] helped to overturn the conventional wisdom concerning the origin of the photovoltage, which had traditionally been thought to be due to a space-charge layer. One explanation[32] invokes a built-in potential difference at the back contact of the semiconductor with the conducting glass. A different explanation involves changes in the Fermi level due to electron injection.[33,34] Both types of mechanisms might play a role.[20]

One important and interesting fact that will contribute toward derivation and subsequent interpretation of the current-voltage characteristics concerns how the experimentally measured recombination current density almost vanishes at short circuit[23]—indicating that the only significant recombination pathway proceeds via back electron transfer into the electrolyte. Indeed, charge recombination between redox species (I_3^- ions) in the electrolyte and conduction-band electrons localized at the nanoporous interface result in suboptimal photovoltage levels—thus limiting the conversion efficiency.[35]

B. Photocurrent-voltage characteristics

We begin by assuming that the number of electrons injected into the conduction band depends only on the incident radiant power—in fact the known very high quantum yields justify this assumption. This assumption allows us to express the recombination current density J_r as a function of the photocurrent density J and the injection current density. Since J_r almost vanishes at short circuit, the injection current equals the short circuit current J_{sc} so that

$$J_r = J_{sc} - J. \tag{1}$$

For a well-mixed solution with identical surface and bulk concentrations (typical for small current densities), the Butler-Volmer equation[36] leads to the following expression for the recombination current density J_r:

$$-J_{\mathrm{r}} = J_0[\exp(-\alpha_C u f \eta) - \exp(\alpha_A u f \eta)], \tag{2}$$

where J_0 denotes the exchange current density, u is the number of electrons transferred in the reaction (and consequently, the order of the rate of reaction for recombination for electrons), α_A and α_C are the anodic and cathodic transfer coefficients, $\eta = V$ is the overpotential, and $f \equiv q/k_B T$.

With some simplification,[23] the widely used[37] Butler-Volmer equation for the recombination current density J_{r} becomes

$$J_{\mathrm{r}} = q k_{\mathrm{et}} c^m n_0^{u\alpha}[\exp(u\alpha q V/k_B T) - 1], \tag{3}$$

where $\alpha = \alpha_A$, u is the number of electrons transferred in the reaction (and consequently, the order of the rate of reaction for recombination for electrons), k_{et} is the back electron transfer rate constant, c is the concentration of the oxidized species, m is the order of the reaction for the oxidized species, q the electronic charge, and n_0 the value in dark conditions of the electron population in the semiconductor. Although one may expect the Butler-Volmer equation itself to fail at the very small scales of the nanopores, yet this last equation correctly describes experimental results.[23] Recall that the actual surface area of the nanocrystalline semiconductor in fact greatly exceeds the nominal area of the device by several orders of magnitude (due to the nanoporous structure). Hence, the injection and recombination currents per unit area of the semiconductor-electrolyte interface at nanoscopic scales always remain much smaller than J_{sc} and J_{r}, respectively.

The Nernst equation for the potential in terms of the concentrations of the oxidized and reduced species holds valid only under equilibrium conditions, yet we know that c varies across the electrolyte. Indeed, since the reduced species greatly exceeds the oxidized species, we can safely conclude that the voltage varies as $\Delta V(x) \approx -(k_B T/q)\ln[c^0/c(x)]$, where $c(x)$ denotes the concentration at a position x across the cell (i.e., electrolyte) and c^0 denotes a reference (or mean) concentration. Nonetheless, we still do not know, *a priori*, exactly how it varies with the potential at the semiconductor-electrolyte interface as the external load (i.e., external impedance) varies due to the out of equilibrium conditions. In this context, one important clue comes from the dependence of the photovoltage on the electron population n. In the semiconductor, injected electrons shift the Fermi level so that $n = n_0 \exp(qV/k_B T)$. This exponential dependence on potential, together with the exponential dependence of c on voltage across the electrolyte, hints at a similar (i.e., exponential) dependence of c on V as the external load varies.

An exponential dependence of c on V would allow us to assume, without loss of generality, the following constitutive equation:

$$\frac{c_{\mathrm{oc}}}{c} = \exp\left[-\frac{q(V - V_{\mathrm{oc}})}{\gamma k_B T}\right]. \tag{4}$$

Here c_{oc} represents the concentration under open circuit conditions and γ represents a free parameter in the model such that γ^{-1} gives the fraction of the voltage variation that affects the oxidized species concentration. Since the tri-iodide concentration cannot vary very much in the liquid, we cannot expect small γ close to equal unity since this would imply $c \propto n$. For now we merely mention that one might naïvely expect $\gamma > 0$ since electron injection and dye regeneration (associated with larger V) produce oxidized species. In fact, we will show below that $\gamma < 0$ and that it bears a relation to the fill factor.

This constitutive equation, Eq. (4), for the electrolyte is consistent with the assumptions of the Butler-Volmer (and Nernst) equations, both of which have their ultimate basis in Boltzmann-Gibbs statistics. Indeed, describing quantitatively the injection and charge separation processes inside the semiconductor requires the use of Fermi-Dirac statistics; however Boltzmann-Gibbs statistics approximates very well the behavior of the electrolyte. But without a constitutive equation, the fill factor remains underdetermined. In this context, the free parameter γ in Eq. (4) will be shown to determine the fill factor by quantifying how the oxidized species concentration varies with the electron population. Notice that the fill factor itself depends on many specific (i.e., nonuniversal) properties of the semiconductor-electrolyte interface, such as composition, morphology, crystallinity, porosity, conductivity, surface properties, and electrolytic conductivity and viscosity. Most if not all of these factors can change the fill factor only by their effects on the recombination current-voltage curve. So we can expect all these factors to affect γ, such that the value of γ will vary from cell to cell, but the crucial point is that we do not expect significant departures from Boltzmann-Gibbs and Fermi-Dirac statistics. Our results reported below clearly demonstrate that the above constitutive equation represents a good first approximation. We find remarkably good agreement with experimental data. The constitutive equation effectively introduces into the model a nonunique characteristic scale of energy that affects the oxidized species, determined by $\gamma k_B T$ (see below).

Moreover, we wish to make clear to the reader not only which physical processes the model takes into account, but also which processes it neglects. We limit our investigations to the charge-exchange processes at the semiconductor-electrolyte interface. Specifically, we do not explicitly take into consideration other parameters of the cell, such as the series resistance of the conducting glass substrate and the platinized counter electrode and the charge-exchange mechanism at the counter electrode. Clearly, such effects alter the photocurrent-voltage curves and may represent nonuniversal aspects of the problem. Nevertheless, we note the following three points: (i) the series resistances make themselves felt strongly only at relatively larger values of the current, i.e., for relatively lower operating voltages; (ii) the effect of an additional series resistance mainly is to lower the short circuit current and to "flatten" the entire curve; (iii) these effects lead to a change in the functional form of the curves, however other preliminary results (not shown here) indicate that the basic shape of the curve remains approximately unchanged.

III. RESULTS

The previous equations immediately lead to an analytical expression for the photocurrent J as a function of the voltage V across the cell

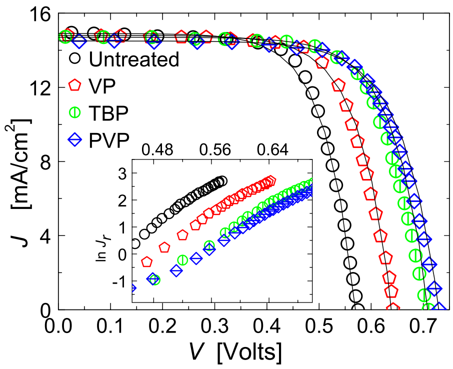

FIG. 1. (Color online) Typical current-voltage characteristics under radiant power of 1.5 a.m., taken from Huang *et al.* (Ref. 23). The four data sets have different characteristics due to varied chemical treatments (see text), yet the theoretical curves (solid lines) corresponding to Eq. (6) can account well for the experimental curves. Inset shows approximate logarithmic relation for the recombination current density J_r versus voltage, consistent with Eq. (3).

$$J=J_{\rm sc}\left\{1-\frac{\exp\left(\dfrac{mq(V-V_{\rm oc})}{\gamma k_BT}\right)}{\exp\left(\dfrac{u\alpha qV_{\rm oc}}{k_BT}\right)-1}\left[\exp\left(\dfrac{u\alpha qV}{k_BT}\right)-1\right]\right\}. \tag{5}$$

Here $m\approx 2$ because of the second-order reaction and $u\alpha \approx 0.7$ according to experimental results.[23,26] We expect this analytical expression to apply to all dye-sensitized solar cells.

We can further simplify Eq. (5) for the photocurrent-voltage relation by making additional realistic assumptions. Equation (3) for the recombination has validity in the large voltage ($V > 80$ mV) regime.[23,26] Below this potential, the recombination current becomes negligible and uninteresting. For any useful cell, $n \gg n_0$ by many orders of magnitude in this regime. So we can approximate Eq. (5) with

$$J=J_{\rm sc}\left[\frac{\exp(V_{\rm oc}/V_{\rm s})-\exp(V/V_{\rm s})}{\exp(V_{\rm oc}/V_{\rm s})-1}\right], \tag{6}$$

where the potential

$$V_{\rm s}\equiv(k_BT/q)\frac{1}{u\alpha+m/\gamma}\approx\frac{1}{40(0.7+2/\gamma)}\text{Volts}, \tag{7}$$

represents a characteristic scale of the exponential decay. Specifically, $V_{\rm s}$ quantifies the photovoltage drop corresponding to a decrease in recombination current density by a factor of $1/e$, where e here denotes Euler's number. Equations (5) and (6) represent the first of three results of this article. Note that for fixed $V_{\rm oc}$ and $J_{\rm sc}$, there is a single free parameter, viz., $V_{\rm s}$ (or, equivalently, γ), which quantifies properties of more fundamental physical mechanisms of transport in the liquid.

We next compare theory and experiment. Figure 1 compares the model with previously reported photocurrent-voltage curves[23] of untreated and pyridine derivative-treated $[\mathrm{RuL_2(NCL)_2}]$-coated nanocrystalline $\mathrm{TiO_2}$ electrodes in $\mathrm{CH_3CN/MNO}$ (50:50 wt %) containing Li(0.3M) and $\mathrm{I_2}$ (30 mM), for a radiant power of 100 mW/cm^2 (AM 1.5). The electrodes had treatment with following substances: 3-vinylpyridine (VP), 4-*tert*-butylpyridine (TBP), and poly(2-vinylpyridine) (PVP). The good agreement with the data validates the model represented by Eqs. (5) and (6). Estimated values of $V_{\rm s}$: 0.0575 (untreated), 0.0615 (VP), 0.0651 (TBP), and 0.0682 V (PVP). Notice that $V_{\rm s}$ changes the fill factor (via γ). A value $V_{\rm s}\to\infty$ (corresponding to purely resistive or ohmic behavior[38]) leads to FF=1/4, whereas $V_{\rm s}\to 0$ leads to unity fill factor—perfect but theoretically impossible except at $T=0$ K. Most dye-sensitized solar cells have FF=0.6–0.7 (Fig. 1).

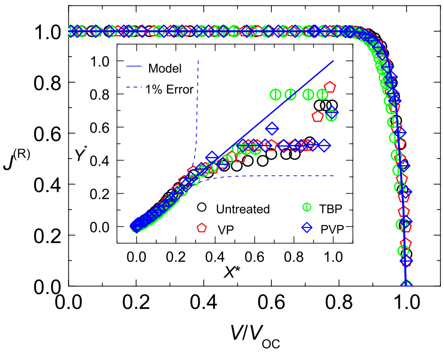

FIG. 2. (Color online) Renormalized photocurrent $J^{(R)}$ versus $V/V_{\rm oc}$ for the curves shown in Fig. 1. The data collapse onto a single universal function stable over a variety of chemical treatments. We have chosen the plotting parameter $v_{\rm s}=1/40$, based on the value of k_BT at room temperature, for illustration (corresponding to our estimate of an upper bound for fill factors). However, data collapse for arbitrary $v_{\rm s}$. Indeed, we can linearize the curves (inset, see text). The dashed line traces the upper and lower uncertainties corresponding to an error of 1% in the short circuit current. Notice how remarkably the data collapse onto a straight line (within 1% tolerance).

We now turn our attention to the question of whether a single universal current-voltage relation can describe all $\mathrm{TiO_2}$ solar cells. According to the theory presented above, all dye-sensitized solar cells must satisfy Eq. (5) if not Eq. (6). If we renormalize the photovoltage to obtain an adimensional measure $V^*\equiv V/V_{\rm oc}$, then every single dye-sensitized solar cell must satisfy the following relation for an idealized renormalized photocurrent:

$$J^{(R)}\equiv\frac{1-[1-(J/J_{\rm sc})(1-\exp(-V_{\rm oc}/V_{\rm s}))]^{V_{\rm s}/V_{\rm oc}v_{\rm s}}}{1-\exp(-1/v_{\rm s})}. \tag{8}$$

Here the plotting parameter $v_{\rm s}$ fixes the shape or fill factor of the renormalized photocurrent. Figure 2 shows the predicted data collapse. We have chosen a value $v_{\rm s}=1/40$ due to its significance for an idealized solar cell with maximum FF (see below) at room temperature. However, we can obtain data collapse for any $v_{\rm s}$ (not shown). Note that $v_{\rm s}$ is not a parameter of the model. This is perhaps more clear if we linearize the curves. We define adimensional coordinates

$$X^*\equiv 1-V/V_{\rm oc},$$

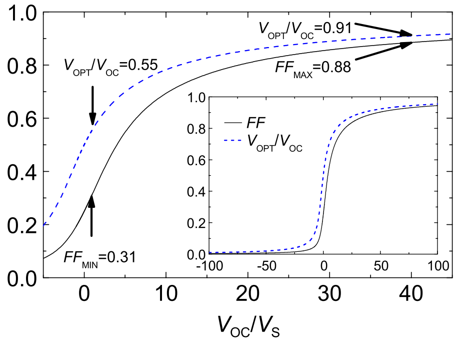

FIG. 3. (Color online) Theoretically predicted fill factors FF and ratio $V_{\mathrm{OPT}}/V_{\mathrm{oc}}$ of optimal operating voltage V_{OPT} to open circuit voltage V_{oc} versus $V_{\mathrm{oc}}/V_{\mathrm{s}}$, where V_{s} represents a characteristic voltage [see Eq. (7)]. We estimate a worst-case lower bound on the fill factor using $V_{\mathrm{oc}}/V_{\mathrm{s}}=1$, and an idealized upper bound using $V_{\mathrm{oc}}/V_{\mathrm{s}}=40$. Inset shows more complete picture (including negative, unphysical $V_{\mathrm{oc}}/V_{\mathrm{s}}$) of the numerical solution of the relevant transcendental equation.

$$Y^* \equiv - V_{\mathrm{s}}/V_{\mathrm{oc}} \;\ln\left\{1 - \frac{J}{J_{\mathrm{sc}}}[1 - \exp(- V_{\mathrm{oc}}/V_{\mathrm{s}})]\right\}. \qquad (9)$$

Note how the data collapse (inset), within remarkably small tolerances.

We next consider the problem from the point of view of scale-invariance symmetry. The fill factor cannot depend on J_{sc} since it cancels in the power ratio. It also remains invariant under a scale transformation $V_{\mathrm{oc}} \to \lambda V_{\mathrm{oc}}$ and $V_s \to \lambda V_s$. In fact, no dilation can alter a ratio of geometric areas. The invariance of FF for arbitrary λ implies that FF can depend on V_{oc} and V_{s} only via their ratio: $\mathrm{FF}=\mathrm{FF}(V_{\mathrm{oc}}/V_{\mathrm{s}})$. The exact functional dependence appears to involve a transcendental equation. Figure 3 shows numerically solved FF as a function of $V_{\mathrm{oc}}/V_{\mathrm{s}}$.

IV. DISCUSSION AND CONCLUSION

We comment on the values typically found for V_{s} and their physical significance. They correspond to $\gamma \approx -6 < 0$. The finding of negative γ suggests that the concentration of redox species (I_3^- ions) decreases with the photovoltage. This may at first seem counterintuitive. Indeed, higher voltage suggests larger electron population and more injection. Moreover, the regeneration of the dye creates I_3^- species, in the proportion of one ion for every two electrons injected. So do we face an apparent inconsistency? In fact, very small recombination current $J_{\mathrm{r}} \approx 0$ under short circuit conditions hints at the correct explanation: the rate of regeneration of the oxidized dye depends not on the photovoltage (almost zero under short circuit) but rather on the rate of electron injection—thus on radiant power. We also know that $c \sim n^{1/\gamma}$ so c scales with n with a fractional power-law scaling exponent ($1/\gamma \approx -1/6$). The fractional power-law behavior might indicate a relevant role for reaction-diffusion processes involving anomalous transport and diffusion. We have already mentioned earlier the inadequacy of the unmodified Butler-Volmer equation at nanoscopic scales. Although such issues lie beyond the present scope, we wish to stress that a negative value of γ should not surprise the reader. Indeed, negative values of γ agree with the expectation of a smaller depletion layer for larger external current drain. Crucially, larger electron population n leads to greater recombination, which consumes the oxidized species and lowers c. Such an inverse relation between n and c requires $\gamma < 0$.

We next comment on the usefulness of the proposed model, noting that it is linearizable via Eq. (9). Our findings yield predictions and in fact allow us to estimate lower and upper limits for FF. Ohmic behavior corresponds to $V_{\mathrm{s}} \to \infty$ and $\mathrm{FF}=1/4$; however such a low value would render a device practically useless. For any useful device, the largest conceivable value of V_{s} should not exceed V_{oc}, which gives us a lower bound for FF of $\mathrm{FF}=0.31$ and an optimal operational voltage of $V_{\mathrm{OPT}}=0.55\ V_{\mathrm{oc}}$. By considering $V_{\mathrm{s}}/V_{\mathrm{oc}}=1/40$ and idealizing $u\alpha=1$ (i.e., no variation in c with external load), we arrive at a theoretical upper bound of FF $=0.88$ and $V_{\mathrm{OPT}}=0.91\ V_{\mathrm{oc}}$, as shown in Fig. 3. For $u\alpha=0.7$ and $\gamma \to \infty$ we obtain slightly smaller FF. Overall, we find excellent agreement with experimental values.

Finally, our findings can explain the physical origin of the large fill factors of dye solar cells. The recombination current becomes insignificant as soon as the voltage drops to $V = V_{\mathrm{oc}} - V_{\mathrm{s}}$ [Eqs. (3) and (6)]. Since $V_{\mathrm{s}} \ll V_{\mathrm{oc}}$, therefore the photocurrent jumps from zero to close to its short circuit value even if the voltage only drops slightly (i.e., by V_{s}). Notice from Fig. 3 that increases in V_{oc}—e.g., due to greater radiant power—should indeed lead to higher FF if V_{s} varies much less than V_{oc}, as in fact occurs. Further analysis of more recent experimental data (not shown here) agrees with the results reported here, although the agreement becomes less good for extremely inefficient cells (as expected).

In summary, our theoretical results (Fig. 3) allow the estimation of FF from $V_{\mathrm{oc}}/V_{\mathrm{s}}$ or vice versa. Moreover, from just three data points, one can reconstruct the entire current-voltage curve via Eq. (6). For known open circuit voltage and short circuit current density, the proposed linearizable model has a single free parameter, corresponding to FF.

ACKNOWLEDGMENTS

We thank BNB (Process No. 2004/ETENE–227), CAPES, CNPq (Process No. 201809/2007-9), and NSF (Grant No. INT-0336343) for partial funding. We thank N. Kumar and M. G. E. da Luz for helpful suggestions, and also I. M. Gléria, A. S. Gonçalves, M. L. Lyra, S. B. Manamohanan, M. R. Meneghetti, S. M. P. Meneghetti, F. A. B. F. de Moura, A. F. Nogueira, L. S. Roman, and E. C. Silva for discussions. G.M.V. thanks V. M. Kenkre and the Consortium of the Americas for Interdisciplinary Science for its hospitality.

[1] H. E. Stanley, Rev. Mod. Phys. **71**, S358 (1999).

[2] H. E. Stanley, *Introduction to Phase Transitions and Critical Phenomena* (Oxford University Press, Oxford, New York, 1971).

[3] H. E. Stanley, L. A. N. Amaral, S. V. Buldyrev, A. L. Goldberger, S. Havlin, H. Leschhorn, P. Maass, H. Makse, C.-K. Peng, M. A. Salinger, M. H. R. Stanley, and G. M. Viswanathan, Physica A **231**, 20 (1996).

[4] V. M. Kenkre, in *Statistical Mechanics and Statistical Methods in Theory and Application*, edited by U. Landman (Plenum, New York, 1977); V. M. Kenkre, E. W. Montroll, and M. F. Shlesinger, J. Stat. Phys. **9**, 45 (1973).

[5] R. Metzler and J. Klafter, Phys. Rep. **339**, 1 (2000); R. Metzler and J. Klafter, J. Phys. A **37**, R161 (2004).

[6] *Lévy Flights and Related Topics in Physics*, edited by M. F. Shlesinger, G. M. Zaslavsky, and U. Frisch (Springer, Berlin, 1995).

[7] E. Barkai, R. Metzler, and J. Klafter, Phys. Rev. E **61**, 132 (2000).

[8] S. V. Buldyrev, S. Havlin, A. Ya. Kazakov, M. G. E. da Luz, E. P. Raposo, H. E. Stanley, and G. M. Viswanathan, Phys. Rev. E **64**, 041108 (2001).

[9] J. C. Cressoni, Marco Antonio Alves da Silva, and G. M. Viswanathan, Phys. Rev. Lett. **98**, 070603 (2007).

[10] J. Nelson, Phys. Rev. B **59**, 15374 (1999).

[11] R. N. Mantegna and H. E. Stanley, *An Introduction to Econophysics* (Cambridge University Press, Cambridge, 2000).

[12] A. L. Barabasi and R. Albert, Science **286**, 509 (1999); R. Albert and A. L. Barabasi, Rev. Mod. Phys. **74**, 47 (2002).

[13] G. M. Viswanathan, V. Afanasyev, S. V. Buldyrev, E. J. Murphy, P. A. Prince, and H. E. Stanley, Nature (London) **381**, 413 (1996); G. M. Viswanathan, S. V. Buldyrev, S. Havlin, M. G. da Luz, E. Raposo, and H. E. Stanley, *ibid.* **401**, 911 (1999).

[14] F. Bartumeus, J. Catalan, U. L. Fulco, M. L. Lyra, and G. M. Viswanathan, Phys. Rev. Lett. **88**, 097901 (2002); E. P. Raposo, S. V. Buldyrev, M. G. E. da Luz, M. C. Santos, H. E. Stanley, and G. M. Viswanathan, *ibid.* **91**, 240601 (2003).

[15] P. Ch. Ivanov, M. G. Rosenblum, C.-K. Peng, H. E. Stanley, and A. L. Goldberger, Nature (London) **383**, 323 (1996).

[16] H. D. Jennings and P. Ch. Ivanov, A. M. Martins, P. C. Silva, and G. M. Viswanathan, Physica A **336**, 585 (2004).

[17] H. Scher and E. W. Montroll, Phys. Rev. B **12**, 2455 (1975).

[18] I. M. Sokolov, Phys. Rev. E **63**, 011104 (2000).

[19] B. O' Regan and M. Grätzel, Nature (London) **353**, 737 (1991).

[20] M. Grätzel, Nature (London) **414**, 338 (2001).

[21] S. M. Sze, *Physics of Semiconductor Devices* (Wiley, New York, 1981); D. A. Fraser, *The Physics of Semiconductor Devices* (Clarendon, Oxford, 1990); G. Burns, *Solid State Physics* (Academic, New York, 1985).

[22] H. J. Snaith and M. Grätzel, Appl. Phys. Lett. **89**, 262114 (2006).

[23] S. Y. Huang, G. Schlichthörl, A. J. Nozik, M. Grätzel, and A. J. Frank, J. Phys. Chem. B **101**, 2576 (1997).

[24] W. A. Gazotti, A. F. Nogueira, E. M. Girotto, M. C. Galazzi, and M.-A. De Paoli, Synth. Met. **108**, 151 (2000); A. F. Nogueira, J. R. Durrant, and M. A. Paoli, Adv. Mater. **13**, 826 (2001); L. S. Roman, M. Berggren, and O. Inganäs, Appl. Phys. Lett. **75**, 3557 (1999).

[25] H. J. Snaith, L. Schmidt-Mende, M. Grätzel, and M. Chiesa, Phys. Rev. B **74**, 045306 (2006).

[26] S. K. Deb, S. Ferrere, A. J. Frank, B. A. Gregg, S. Y. Huang, A. J. Nozik, Z. Schlichthörl, and A. Zaban, Conf. Rec. IEEE Photovoltaic Spec. Conf. **26**, 507 (1997).

[27] J. R. Durrant, J. Nelson, and D. R. Klug, Mater. Sci. Technol. **16**, 1345 (2000).

[28] N. Kopidakis, K. D. Benkstein, J. van de Lagemaat, A. J. Frank, Q. Yuan, and E. A. Schiff, Phys. Rev. B **73**, 045326 (2006).

[29] J. van de Lagemaat, N. Kopidakis, N. R. Neale, and A. J. Frank, Phys. Rev. B **71**, 035304 (2005).

[30] N. J. Cherepy, G. P. Smestad, M. Grätzel, and J. Z. Zhang, J. Phys. Chem. B **101**, 9342 (1997).

[31] G. Hodes, I. D. J. Howell, and L. M. Peter, J. Electrochem. Soc. **139**, 3136 (1992).

[32] K. Schwarzburg and F. Willig, J. Phys. Chem. B **103**, 5743 (1999).

[33] F. Pichot and B. A. Gregg, J. Phys. Chem. B **104**, 6 (2000).

[34] D. Cahen, G. Hodes, M. Grätzel, J. F. Guillemoles, and I. Riess, J. Phys. Chem. B **104**, 2053 (2000).

[35] A. Stanley and D. Matthews, Aust. J. Chem. **48**, 1293 (1995); G. Smestad, Sol. Energy Mater. Sol. Cells **32**, 273 (1994); P. Liska, Ph.D. Thesis, Swiss Federal Institute of Technology, 1994.

[36] A. J. Bard and L. R. Faulkner, *Electrochemical Methods* (Wiley, New York, 1980); A. Wieckowski, *Interfacial Electrochemistry: Theory, Experiment, and Applications* (CRC, Boca Raton, 1999).

[37] L. M. Peter, Phys. Chem. Chem. Phys. **9**, 2630 (2007); P. J. Cameron, L. M. Peter, and S. Hore, J. Phys. Chem. B **109**, 930 (2005); P. J. Cameron and L. M. Peter, *ibid.* **109**, 7392 (2005).

[38] J. S. Agnaldo, J. B. V. Bastos, J. C. Cressoni, and G. M. Viswanathan, Revista Brasileira de Ensino de Física **28**, 77 (2006).